Trop J Nat Prod Res, October 2025; 9(10): 4803 - 4811 **ISSN 2616-0684 (Print)**
ISSN 2616-0692 (Electronic)

Tropical Journal of Natural Product Research

Available online at https://www.tjnpr.org

Original Research Article

Green-Synthesized Silver Nanoparticles from Acalypha godseffiana and Their Biofilm-Disruptive Activity against ESKAPE Pathogens

Safiyya M Shehu[1], Shamsuddeen Umar,[2] Sandeep Sharma[3], Sarika Sharma[1]*

[1]*Department of Microbiology, School of Bioengineering & Biosciences, Lovely Professional University, Phagwara (Punjab), India*
[2]*Department of Microbiology, Bayero University, Kano, Nigeria.*
[3] *Department of Medical Laboratory Sciences, School of Allied Medical Sciences, Lovely Professional University, Phagwara (Punjab), India*

ARTICLE INFO

Article history:
Received 21 July 2025
Revised 01 October 2025
Accepted 05 October 2025
Published online 01 November 2025

ABSTRACT

The emergence of multidrug-resistant (MDR) pathogens, including the ESKAPE group (*Enterococcus faecium, Staphylococcus aureus, Klebsiella pneumoniae, Acinetobacter baumannii, Pseudomonas aeruginosa,* and *Escherichia coli*), underscores the urgent need for novel antimicrobial agents. This study reports the green synthesis of silver nanoparticles (AgNPs) using *Acalypha godseffiana* leaf extract and evaluates their potent antibiofilm activity against these critical pathogens. UV–Vis spectroscopy confirmed nanoparticle formation through a characteristic surface plasmon resonance peak at 437 nm. In comparison, transmission electron microscopy (TEM) revealed spherical nanoparticles ranging from 1 to 20 nm, stabilized by plant-derived phytochemicals. Energy-dispersive X-ray (EDX) analysis verified the presence of elemental silver with a peak at 3.0 keV, accompanied by organic capping agents. The biosynthesized AgNPs demonstrated dose-dependent inhibition of biofilm formation, exhibiting maximal activity against *S. aureus* (61.71% inhibition at 100 µg/mL) and *A. baumannii* (52.58%). Minimum biofilm eradication concentrations (MBEC) indicated complete disruption of established biofilms at 200 µg/mL for *P. aeruginosa* and 400 µg/mL for *E. faecium*. Mechanistic investigations suggest that the antibiofilm effects are mediated by reactive oxygen species (ROS) generation, degradation of extracellular polymeric substances (EPS), and disruption of bacterial membranes, potentiated by synergistic interactions with flavonoids and phenolic compounds from the plant extract. These findings highlight *A. godseffiana*-derived AgNPs as a sustainable and eco-friendly alternative to conventional antibiotics, particularly for managing biofilm-associated MDR infections. The study provides critical insights and dosage thresholds essential for future translational applications, including medical device coatings and topical antimicrobial formulations.

Keywords: *Acalypha godseffiana, Enterococcus faecium, Staphylococcus aureus, Escherichia coli* pathogens, Antimicrobial resistance.

Introduction

Nanotechnology has profoundly impacted numerous scientific fields, particularly in the development of innovative antimicrobial agents. Among the most extensively studied nanomaterials are silver nanoparticles (AgNPs), renowned for their broad-spectrum antimicrobial activity, high surface-area-to-volume ratio, and distinctive physicochemical properties that facilitate diverse interactions with microbial cells.[1,2] The antimicrobial mechanisms of AgNPs include disruption of bacterial cell membranes, interference with DNA replication, and the induction of oxidative stress via reactive oxygen species (ROS) generation.[3,4]

*Corresponding author. Email: sarika.28186@lpu.co.in
Tel: + 919816535399

Citation: Shehu S M, Umar S, Sharma S, Sharma S. Green-Synthesized Silver Nanoparticles from *Acalypha godseffiana* and Their Biofilm-Disruptive Activity against ESKAPE Pathogens. Trop J Nat Prod Res. 2025; 9(10): 4803 – 4811 https://doi.org/10.26538/tjnpr/v9i10.15

Official Journal of Natural Product Research Group, Faculty of Pharmacy, University of Benin, Benin City, Nigeria

Beyond their bactericidal effects, AgNPs have also demonstrated substantial efficacy in disrupting bacterial biofilms, positioning them as promising candidates for the treatment of persistent and biofilm-associated infections.[5,6] Conventional chemical and physical methods for synthesizing silver nanoparticles (AgNPs) often involve toxic solvents, hazardous reducing agents, and high energy input, raising concerns about environmental sustainability and biomedical safety. To address these challenges, green synthesis approaches have emerged as sustainable and biocompatible alternatives. These methods utilize natural biological systems, particularly plant extracts[7], to reduce silver ions and stabilize nanoparticles under ambient conditions. Plant-mediated synthesis is beautiful due to its simplicity, cost-effectiveness, and the abundance of phytochemicals, such as flavonoids, alkaloids, phenolics, and terpenoids, which can serve dual roles as reducing and capping agents. These bioactive compounds may also enhance the functional properties of AgNPs, contributing synergistically to their antimicrobial activity [8] Despite the growing interest in green nanotechnology, many medicinal and ornamental plants remain underexplored for their nanoparticle-synthesizing potential. *Acalypha godseffiana*, an ornamental plant from the Euphorbiaceae family, is one such example.[9] Preliminary phytochemical studies have identified several secondary metabolites in *A. godseffiana*, including saponins, tannins, flavonoids, and phenolic acids,[10] which are known for their antimicrobial and antioxidant properties. These compounds hold promise for facilitating the green synthesis of nanoparticles.
However, limited research has investigated the use of *A. godseffiana* in nanoparticle synthesis, and its antimicrobial potential in nanoform

remains largely uncharacterized. The clinical relevance of green-synthesized AgNPs becomes increasingly evident in the face of antimicrobial resistance (AMR), a pressing global health challenge. The rise of multidrug-resistant (MDR) bacteria has compromised the efficacy of conventional antibiotics and led to a surge in healthcare-associated infections. Of particular concern are the ESKAPE pathogens, *Enterococcus faecium*, *Staphylococcus aureus*, *Klebsiella pneumoniae*, *Acinetobacter baumannii*, *Pseudomonas aeruginosa*, and *Escherichia coli*,[11] which are responsible for the majority of nosocomial infections and are notorious for their capacity to "escape" antimicrobial treatments via mechanisms such as efflux pumps, enzymatic degradation, and target-site modifications.[12] A key feature of many ESKAPE pathogens is their ability to form biofilms—structured microbial communities embedded within an extracellular polymeric substance (EPS) matrix.[13] Biofilms provide enhanced protection against antimicrobial agents and host immune responses and are commonly associated with chronic infections and medical device-related complications. Within biofilms, bacteria exhibit altered metabolic activity and gene expression, leading to phenotypic resistance even in the absence of genetic mutations.[14] This makes biofilm-associated infections especially challenging to treat and a significant barrier in managing MDR pathogens [15] In light of this challenge, there is increasing interest in developing antimicrobial agents that also possess biofilm-disruptive properties. Silver nanoparticles, especially those synthesized via green methods, offer a promising dual-function approach. The presence of phytochemicals in plant-mediated AgNPs may enhance their interaction with microbial surfaces and EPS components, thereby improving antibiofilm efficacy. This study explores the green synthesis of silver nanoparticles using an aqueous leaf extract of *Acalypha godseffiana*. It evaluates their antibiofilm activity and minimum biofilm eradication concentration (MBEC) against ESKAPE pathogens, including *Escherichia coli*. The synthesized AgNPs are characterized using standard analytical techniques, including ultraviolet-visible (UV-Vis) spectroscopy, scanning electron microscopy (SEM), energy-dispersive X-ray (EDX), and transmission electron microscopy (TEM), to determine their size, morphology, and elemental composition. Their antimicrobial properties are then assessed in both planktonic and biofilm states using clinically relevant ESKAPE strains. By integrating plant-based green nanotechnology with antimicrobial evaluation, this study aims to contribute to the development of sustainable, biologically active nanomaterials capable of addressing the increasing burden of resistant and biofilm-associated infections. The findings also provide insights into the potential of underutilized botanical species in the eco-friendly production of nanotherapeutics with clinical relevance.

Materials and Methods

Chemicals and Equipment

Methanol and silver nitrate, both of analytical grade, were obtained from Ceman Scientific LTD in Nigeria. Standard bacterial strains (ATCC), *Enterococcus faecium* ATCC 700221, *Staphylococcus aureus* (MRSA) ATCC BAA-1720, *Klebsiella pneumoniae* ATCC BAA-1705, *Acinetobacter baumannii* ATCC BAA-1710, *Pseudomonas aeruginosa* ATCC BAA-1744, and *Escherichia coli* ATCC 14714 were acquired from the Microbiology Laboratory at Bayero University, Kano. Deionized, double-distilled water was used to prepare all aqueous solutions. The study employed a mechanical blender, centrifuge, UV–Vis spectrophotometer, SPSS software, incubator, autoclave, sterile 6 mm paper discs, micropipettes, 96-well polystyrene microtiter plates, MHA/MHB, and a biosafety cabinet.

Collection, Identification, and Extraction of Acalypha godseffiana Leaves

Fresh leaves of *Acalypha godseffiana* were collected from the botanical garden of Bayero University, Kano, Nigeria (11.9837° N, 8.4776° E). The plant was taxonomically identified at the university herbarium and assigned the accession number BUKHAN 0352. The leaves were washed thoroughly with tap water, followed by distilled water, to remove surface impurities. They were then cut into small pieces and air-dried at room temperature. Once completely dried, the leaves were ground into a fine powder using a mechanical blender. For extraction, 62.5 g of the powdered leaf material was subjected to Soxhlet extraction using 250 mL of methanol for 3 hours. The resulting extract was concentrated using a rotary evaporator at 40 °C. The concentrated extract was then poured into a petri dish, spread to a uniform thickness of 4–5 mm, and dried in an oven at 50 °C for 18 hours. The dried methanolextract was stored at −4 °C until further use. [16]

Green Synthesis of Silver Nanoparticles

Silver nanoparticles (AgNPs) were synthesized via an eco-friendly method, using the methanolic extract of *Acalypha godseffiana* as both the reducing and stabilizing agent. A 1 mM aqueous solution of silver nitrate ($AgNO_3$, 90 mL) was mixed with 10 mL of the plant extract (1 mg/mL) under continuous magnetic stirring at 1200 rpm for 60 minutes at room temperature. The formation of AgNPs was indicated by a visible color change from pale yellow to dark brown. The resulting colloidal suspension was centrifuged at 6000 rpm for 20 minutes, and this process was repeated three times to ensure thorough purification. The resulting pellet was washed with deionized water and air-dried. The dried nanoparticles were stored and subsequently used for characterization and biological assays.[17]

Characterization of green-synthesized silver nanoparticles

Visual Observation

The formation of silver nanoparticles (AgNPs) was initially monitored through a visible color change in the reaction mixture, indicating the reduction of silver ions (Ag^+) to elemental silver.

UV-Vis spectroscopy

The optical properties of the biosynthesized *Acalypha godseffiana*-mediated AgNPs were analyzed using a double-beam UV–Vis spectrophotometer (LI-2800 Ex, Lambda Scientific, China) over a wavelength range of 200–800 nm. Spectral measurements were recorded at different time intervals to monitor the progression of nanoparticle synthesis, with distilled water used as the reference blank.[18,19]

Scanning Electron Microscopy (SEM) and Energy-Dispersive X-ray Spectroscopy (EDX)

The surface morphology and particle size distribution of the synthesized AgNPs were examined using high-resolution scanning electron microscopy (SEM) (Model: JSM-7600F, JEOL Ltd., Tokyo, Japan). For SEM analysis, AgNPs were dispersed in deionized water (1 mg/mL), sonicated for homogeneity, and a drop of the suspension was placed on a clean glass slide, air-dried, and subsequently sputter-coated with gold. [20] Elemental composition was confirmed through Energy-Dispersive X-ray (EDX) spectroscopy, which provided qualitative and semi-quantitative data on the elemental constituents of the synthesized nanoparticles.[21]

Transmission electron microscopy

The morphological characteristics of the biosynthesized *Acalypha godseffiana*-mediated AgNPs were examined using a transmission electron microscope (JEM-2100, JEOL Ltd., Japan) operated at an accelerating voltage of 200 kV. Before imaging, five milliliters of AgNP colloidal solution were centrifuged twice at 20,000 rpm for 20 minutes to remove unbound molecules. The resulting pellet was re-dispersed in 1 ml of distilled water, and a few drops of the suspension were placed onto a carbon-coated copper grid. The grid was dried in a hot air oven at 60°C for four hours before analysis.[22, 23]

Biofilm Inhibition Assay Using Green-Synthesized Silver Nanoparticles

The inhibitory effects of biosynthesized silver nanoparticles (AgNPs) on biofilm formation were assessed against the same ATCC strains of ESKAPE pathogens using the microtiter plate method. A 96-well sterile microtiter plate was inoculated with 100 µL of bacterial suspensions prepared from overnight cultures of *Enterococcus faecium* ATCC 700221, *Staphylococcus aureus* (MRSA) ATCC BAA-1720, *Klebsiella pneumoniae* ATCC BAA-1705, *Acinetobacter baumannii* ATCC BAA-1710, *Pseudomonas aeruginosa* ATCC BAA-1744, and *Escherichia coli* ATCC 14714. Each well was then treated with 100 µL of AgNPs at

varying concentrations (25, 50, 75, and 100 µg/mL). The plates were incubated at 37 °C for 24 hours to allow biofilm development. After incubation, non-adherent cells were removed by gently washing the wells with sterile distilled water. Adherent biofilms were fixed by staining with 1% crystal violet for 30 minutes, followed by thorough rinsing and decolorization using 95% ethanol. Biofilm biomass was quantified by measuring the absorbance at 590 nm using a microplate reader. [24, 25] The percentage of biofilm inhibition relative to untreated controls was calculated using Equation 1.

$$\%\text{Inhibition} = \left(\text{ODcontrol} - \frac{\text{ODtreated}}{\text{ODcontrol}}\right) \times 100 \text{----------Equation 1}$$

Determination of Minimum Biofilm Eradication Concentration (MBEC)

The Minimum Biofilm Eradication Concentration (MBEC) was determined using a modified 96-well microtiter plate assay, adapted from previously established protocols.[26,27] Briefly, 24-hour-old biofilms of the selected ESKAPE pathogens were established in flat-bottom 96-well polystyrene microtiter plates (Costar, Sigma-Aldrich, USA), as previously described. Following biofilm formation, the wells were gently washed twice with sterile phosphate-buffered saline (PBS, pH 7.4) to remove non-adherent planktonic cells, and subsequently air-dried under sterile conditions.

Serial two-fold dilutions of the test antimicrobial agents, including the green-synthesized silver nanoparticles, were prepared in fresh nutrient broth at concentrations selected based on previously determined MIC values. A total of 200 µL of each dilution was added to the wells containing preformed biofilms. The plates were incubated at 37 °C for 24 hours under static conditions. Post-treatment, the wells were rinsed three times with PBS to remove residual antimicrobial agents. Biofilms were then mechanically disrupted by scraping the well surfaces with sterile pipette tips. The recovered biofilm material was transferred to sterile Eppendorf tubes containing 1 mL of PBS and subjected to ultrasonic treatment in a water bath sonicator (40 kHz) for 10 minutes to enhance the detachment and dispersion of biofilm-embedded cells. Thereafter, 100 µL aliquots from each suspension were plated on Mueller-Hinton agar and incubated at 37 °C for 24 hours. Colony-forming units (CFUs) were enumerated, and the MBEC was defined as the lowest concentration of the antimicrobial agent that resulted in no visible CFU growth. All experiments were conducted in triplicate, and appropriate controls were included: untreated biofilms (positive control) and media-only wells (negative control).

Statistical analysis

All experiments were carried out in triplicate for each of the four different concentrations tested. Data were analyzed using the SPSS software package for Windows. Results were expressed as mean ± standard deviation (SD). One-way analysis of variance (ANOVA) was performed to assess the significance of differences among groups. A p-value of less than 0.05 was considered statistically significant.

Results and Discussion

Green synthesis of silver nanoparticles

A distinct color change in the reaction mixture initially indicated the formation of silver nanoparticles (AgNPs). Upon the addition of *Acalypha godseffiana* leaf extract to a one mM silver nitrate ($AgNO_3$) solution, the solution color shifted from colorless to golden brown (Fig. 1A). This color change signifies the reduction of silver ions (Ag^+) to elemental silver (Ag^0), a hallmark of nanoparticle formation in green synthesis protocols. The brown coloration arises from surface plasmon resonance (SPR), a phenomenon associated with the collective oscillation of electrons on the surface of silver nanoparticles in response to light. To confirm nanoparticle formation, UV–Visible spectroscopy was performed. The absorption spectrum exhibited a pronounced peak at approximately 437 nm (Fig. 1B), characteristic of the SPR band of AgNPs. This peak confirms the presence of colloidal silver nanoparticles and supports the visual observation. Furthermore, the sharpness and position of the SPR peak suggest the formation of small, well-dispersed nanoparticles. These findings validate the efficacy of *A. godseffiana* extract as a reducing and stabilizing agent for the green synthesis of silver nanoparticles.[28]

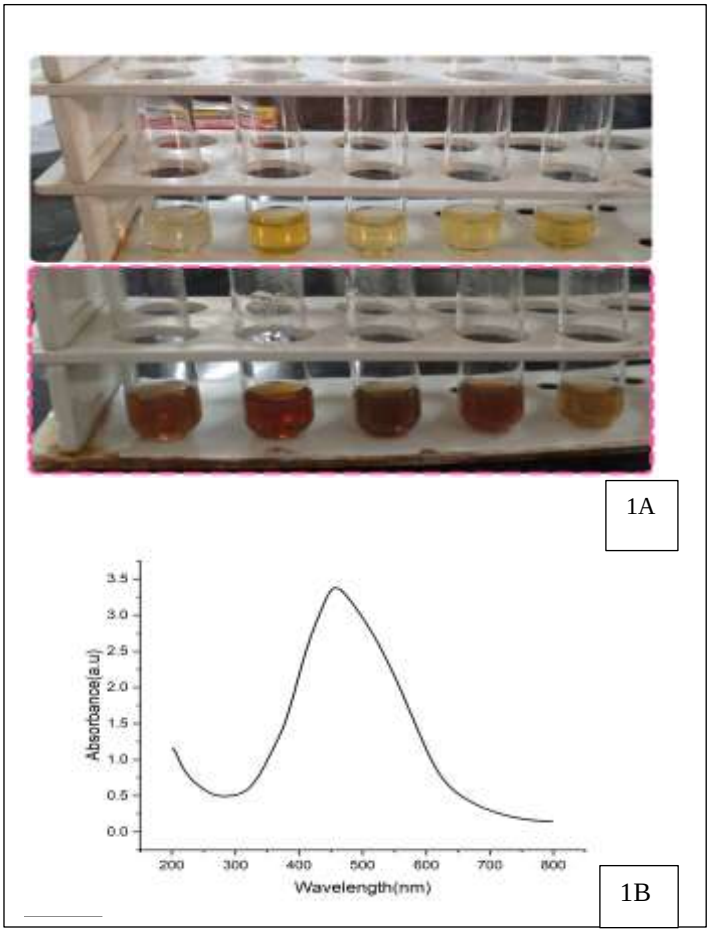

Figure 1: (A) Visual inspection of color change as AgNPs are synthesized, (B) UV–visible spectra of AgNPs.

Scanning Electron Microscopy (SEM) Analysis

The SEM analysis revealed a heterogeneous surface morphology characterized by irregularly shaped and aggregated particles dispersed over a rough and uneven matrix (Fig. 2A–2C). Although silver nanoparticles are conventionally expected to be spherical, the synthesized AgNPs displayed significant agglomeration and non-uniformity in shape. These are likely due to the presence of phytochemicals from *Acalypha godseffiana* extract acting as natural reducing and stabilizing agents. Some rounded structures were visible; however, their fused or embedded appearance suggests poor dispersion and potential structural deformation, likely arising from particle coalescence during synthesis.[29] These morphological features indicate a partially crystalline structure, commonly observed in green-synthesized nanoparticles mediated by plant-derived biomolecules.

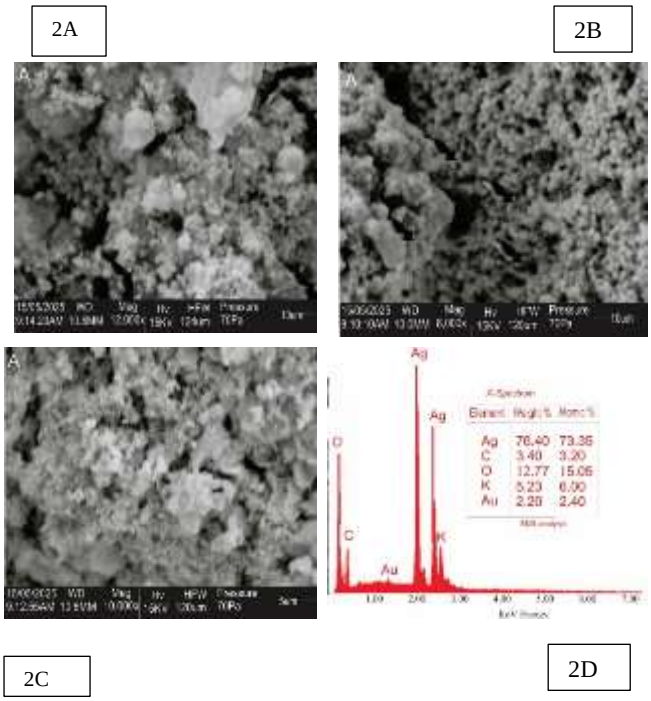

Figure 2: Scanning Electron Microscopy (SEM) images and EDX of silver nanoparticles synthesized using *A. godseffiana* extract

Scanning Electron Microscopy (SEM) images of silver nanoparticles synthesized using *A. godseffiana* extract, shown at different magnifications: (A) 8,000×, (B) 12,000×, and (C) 10,000×. The images reveal aggregated, irregularly shaped particles distributed across a rough surface, with evidence of particle fusion and limited dispersion, likely due to the presence of phytochemical capping agents from the plant extract. (C) EDX of AgNPs

Similar aggregation patterns have been reported in AgNPs synthesized using other plant extracts, where compounds such as flavonoids, phenolics, and proteins are implicated in promoting particle fusion and irregular shapes. While aggregation may reduce surface area and influence the colloidal stability of the nanoparticles, it may also enhance biocompatibility and reduce cytotoxicity—desirable features for biomedical applications. Overall, the SEM findings support the involvement of *A. godseffiana* phytoconstituents in the synthesis and stabilization of AgNPs, highlighting their role in shaping nanoparticle morphology during the green synthesis process.

Energy Dispersive X-ray (EDX) Analysis

The EDX spectrum of the biosynthesized silver nanoparticles confirmed the presence of elemental silver through a characteristic strong peak around 3.0–3.2 keV (Fig. 2D), validating the successful reduction of Ag^{+} to Ag^{0}. In addition to silver, signals corresponding to elements such as carbon (C), oxygen (O), phosphorus (P), sulfur (S), potassium (K), calcium (Ca), and chlorine (Cl) were also detected. These elements likely originate from phytochemicals present in the *Acalypha godseffiana* extract, which acted as natural reducing and stabilizing agents during the synthesis process. The detection of chlorine suggests the potential formation of silver chloride (AgCl) as a minor secondary phase, consistent with XRD findings.[30] The presence of other plant-derived elements indicates effective bio-capping of the nanoparticles by secondary metabolites such as phenolics, flavonoids, and proteins. These findings are in line with earlier reports on green synthesis of AgNPs, where residual plant-based biomolecules are commonly observed on the nanoparticle surface.[31] The organic capping not only stabilizes the particles but may also enhance their interaction with microbial membranes, contributing to the observed antimicrobial activity. Overall, the EDX analysis supports the role of *A. godseffiana* phytochemicals in nanoparticle formation, capping, and functional performance.[32,33]

Transmission Electron Microscopy (TEM) Analysis

Transmission Electron Microscopy (TEM) images (Fig. 3A–C) revealed the successful synthesis of silver nanoparticles (AgNPs) with predominantly spherical morphology and a narrow size distribution. The nanoparticles were uniformly dispersed with minimal aggregation, and their sizes ranged from approximately 1.47 nm to 5.80 nm. At lower magnification (Fig. 3A), the particles appeared well distributed, with the majority measuring below 20 nm, indicating efficient nanoscale synthesis. Higher magnification images (Fig. 3B–C) confirmed these size estimates and showed well-defined particle boundaries, further supporting the crystalline and monodispersed nature of the AgNPs.

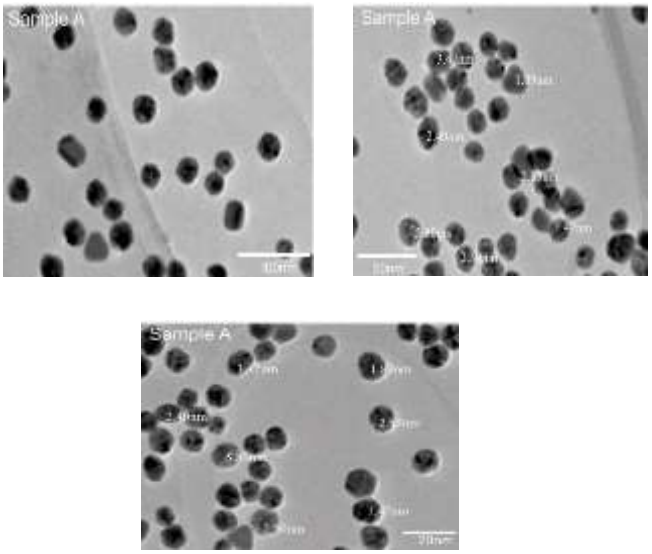

Figure 3: Transmission Electron Microscopy (TEM) images of silver nanoparticles synthesized using *A. godseffiana* extract, shown at different magnifications: (A) 100nm, (B) 50nm, and (C) 20nm.

Although minor clustering was observed in certain regions, most particles maintained discrete boundaries without significant fusion. These suggest the presence of phytochemicals from *Acalypha godseffiana* acting as natural capping and stabilizing agents during the synthesis process. The small particle size and predominantly spherical shape are consistent with previous reports on green-synthesized AgNPs, where plant-derived compounds such as flavonoids and tannins play a critical role in controlling nucleation, preventing overgrowth, and stabilizing the nanoparticles.[34]

The ultrasmall dimensions observed, particularly within the 2–4 nm range, are noteworthy, as they offer a high surface area-to-volume ratio and enhanced biological reactivity. These features are advantageous for antimicrobial applications. These morphological characteristics, combined with the absence of irregular shapes or large aggregates, further underscore the effectiveness of the biosynthetic route employed. Additionally, the high degree of uniformity and dispersity among the nanoparticles reflects a well-regulated green synthesis process that successfully balances the reduction of silver ions with stabilization by phytochemicals from *Acalypha godseffiana* [35]

Similar trends have been reported in AgNPs synthesized from other medicinal plants, where nanoparticle properties were strongly influenced by the type and concentration of capping phytochemicals.[36] The findings in this study further reinforce that *A. godseffiana* extract

functions not only as a reducing agent but also as an effective stabilizer, contributing to the consistent size and spherical morphology of the synthesized nanoparticles. Overall, the TEM analysis confirms the successful biosynthesis of highly uniform, ultrasmall AgNPs, highlighting their suitability for biomedical and antimicrobial applications[37]

Antibiofilm Activity of green-synthesized AgNPs

The antibiofilm activity of AgNPs was assessed against all test strains using OD_{590} measurements and corresponding percent inhibition values. An apparent concentration-dependent inhibition of biofilm formation was observed across all strains. The highest inhibition occurred at 100 µg/mL AgNPs, with *Staphylococcus aureus* MRSA showing 61.71% inhibition and *Acinetobacter baumannii* exhibiting 52.58%. Although *Pseudomonas aeruginosa* and *Enterobacter* spp. Demonstrated strong baseline biofilm production (OD_{590} Control ~1.15), AgNP treatment still led to substantial inhibition (48.50% and 42.59%, respectively, at 100 µg/mL). The lowest inhibition levels were recorded for *Klebsiella pneumoniae* (43.56%) and *Enterococcus faecium* (39.60%) (Table 1; Fig. 4).

Table 1: Percentage biofilm inhibition by AgNPs (25–100 µg/mL) across ESKAPE pathogens. Data represent mean inhibition values based on OD_{590} readings.

Pathogen	AgNPs Conc. (µg/mL)	OD_{590} (Mean ± SD)	% Inhibition
Enterococcus faecium	0 (Control)	0.1843 ± 0.01	0.00%
	100	0.0970 ± 0.06	47.38%
	75	0.1333 ± 0.01	27.71%
	50	0.1213 ± 0.02	34.18%
	25	0.1843 ± 0.01	0.00%
Staphylococcus aureus	0 (Control)	0.175 ± 0.01	0.00%
	100	0.067 ± 0.02	61.71%
	75	0.097 ± 0.03	44.57%
	50	0.122 ± 0.02	30.29%
	25	0.131 ± 0.02	25.14%
Klebsiella pneumonia	0 (Control)	0.143 ± 0.01	0.00%
	100	0.081 ± 0.04	43.56%
	75	0.095 ± 0.02	33.57%
	50	0.122 ± 0.004	14.69%
	25	0.138 ± 0.01	3.50%
Acinetobacter baumannii	0 (Control)	0.1735 ± 0.01	0%
	100	0.0823 ± 0.03	52.58%
	75	0.0967 ± 0.02	44.26%
	50	0.1273 ± 0.01	26.63%
	25	0.1377 ± 0.01	20.66%
Pseudomonas aeruginosa	0 (Control)	0.1915 ± 0.04	0%
	100	0.0757 ± 0.05	48.50%
	75	0.1030 ± 0.05	29.93%
	50	0.1250 ± 0.01	15.01%
	25	0.1197 ± 0.01	18.59%
Escherichia coli	0 (Control)	0.9715 ± 0.04	0%
	100	0.1083 ± 0.05	42.59%
	75	0.1657 ± 0.08	12.19%
	50	0.1657 ± 0.04	12.19%
	25	0.1590 ± 0.02	15.76%

ISSN 2616-0684 (Print)
ISSN 2616-0692 (Electronic)

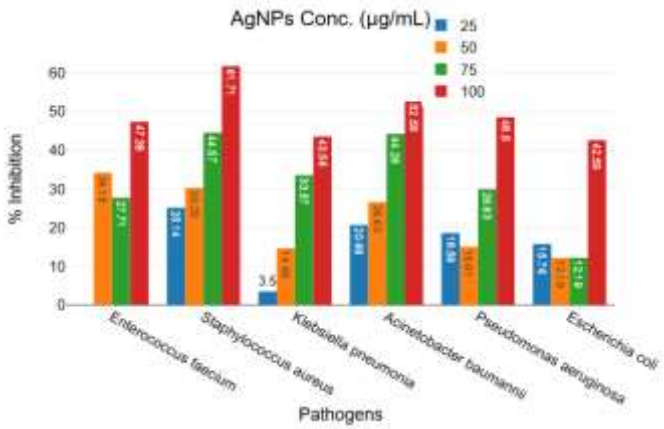

Figure 4: Percentage Biofilm Inhibition by AgNPs (25–100 µg/mL) Across ESKAPE Pathogens

Bar chart showing mean percentage inhibition of biofilm formation by green-synthesized AgNPs at increasing concentrations (25–100 µg/mL) across six ESKAPE pathogens. Inhibition was calculated based on OD_{590} absorbance values. The data indicate a concentration-dependent response, with *S. aureus* and *A. baumannii* showing the highest susceptibility. These findings demonstrate that green-synthesized AgNPs possess dose-dependent antibiofilm activity against both Gram-positive and Gram-negative multidrug-resistant strains. The observed inhibition aligns with recent studies suggesting that AgNPs disrupt biofilm formation by interfering with bacterial quorum sensing, inhibiting extracellular polymeric substance (EPS) production, and increasing cell membrane permeability.[38] Since biofilms contribute significantly to antimicrobial resistance by shielding bacteria from host defenses and antibiotics,[39] such disruption is of considerable therapeutic value. The more potent inhibition observed in *S. aureus* MRSA and *A. baumannii* may be due to differences in cell wall composition or biofilm architecture. In contrast, the lower inhibition in *K. pneumoniae* and *E. faecium* could be linked to denser EPS matrices or intrinsic resistance mechanisms.[40] In summary, the results support the potential of green-synthesized AgNPs as effective antibiofilm agents, especially against multidrug-resistant pathogens. Their dual antimicrobial and antibiofilm activities suggest promising applications in biomedical settings, such as coatings for medical devices, wound dressings, and adjunctive treatments for chronic or device-associated infections.[41] These properties position AgNPs as valuable candidates in the ongoing battle against antimicrobial resistance.

Minimum Biofilm Eradication Concentration (MBEC)

The Minimum Biofilm Eradication Concentration (MBEC) of the synthesized silver nanoparticles (AgNPs) was evaluated to determine the lowest concentration required to eliminate mature biofilms (CFU = 0) with no observable regrowth. As shown in Table 2, AgNPs exhibited concentration-dependent eradication activity against all tested bacterial pathogens. *Pseudomonas aeruginosa* was the most susceptible strain, with complete biofilm eradication achieved at 200 µg/mL. Moderate susceptibility was observed in *Staphylococcus aureus*, *Klebsiella pneumoniae*, and *Acinetobacter baumannii*, each with MBEC values of 300 µg/mL. In contrast, *Enterococcus faecium* and *Escherichia coli* required higher concentrations (400 µg/mL) for complete eradication of their biofilms.

Table 2: Minimum Biofilm Eradication Concentration (MBEC) of synthesized silver nanoparticles against biofilms of ESKAPE pathogens.

Pathogen	Max Inhibition @100 µg/mL	AgNP Conc. (µg/mL)	log CFU/mL before treatment	log CFU/mL after treatment	Log Reduction	MBEC (µg/mL) >99.99%	Regrowth Observed (Y/N)
Enterococcus faecium	39.6%	100	8	8	0	—	Yes
		150	8	7	1	—	Yes
		200	8	6	2	—	Yes
		250	8	5	3	—	Yes
		300	8	2	6	—	Yes
		400	8	0	8	400	No
Staphylococcus aureus	61.71%	100	8	8	0	—	Yes
		150	8	6	2	—	Yes
		200	8	5	3	—	Yes
		250	8	2	6	—	Yes
		300	8	0	8	300	No
Klebsiella pneumonia	43.56%	100	8	7	1	—	Yes
		150	8	6	2	—	Yes
		200	8	5	3	—	Yes

		250	8	1	7	—	Yes
		300	8	0	8	300	No
Acinetobacter baumannii	52.58%	100	8	8	0	—	Yes
		150	8	5	3	—	Yes
		200	8	5	3	—	Yes
		250	8	2	6	—	Yes
		300	8	0	8	300	No
Pseudomonas aeruginosa	48.5%	100	8	6	2	—	Yes
		150	8	5	3	—	Yes
		200	8	0	8	200	No
		250	8	0	8	200	No
Escherichia coli	42.6%	100	8	8	0	—	Yes
		150	8	7	1	—	Yes
		200	8	6	2	—	Yes
		250	8	5	3	—	Yes
		300	8	2	6	—	Yes
		400	8	0	8	400	No

These results highlight that the antibiofilm efficacy of AgNPs is both strain-dependent and influenced by the structural and physiological properties of the bacterial species. The higher susceptibility of *P. aeruginosa* may be attributed to its relatively thinner extracellular polymeric substance (EPS) matrix and increased sensitivity to reactive oxygen species (ROS) generated by AgNPs.[42] Conversely, the more resistant nature of *E. faecium* and *E. coli* biofilms likely stems from their denser and more complex EPS architecture, which acts as a formidable barrier to nanoparticle penetration and antimicrobial action.[43] Overall, these findings demonstrate that green-synthesized AgNPs possess potent antibiofilm activity against both Gram-positive and Gram-negative pathogens. However, higher concentrations may be required for strains with more robust biofilm-forming capabilities. The ability of AgNPs to disrupt and eradicate mature biofilms reinforces their promise as alternative or adjunctive agents in the management of biofilm-associated infections, particularly in settings where conventional antibiotics fail due to resistance.

Statistical Analysis of Antibiofilm Activity

To evaluate the significance of the inhibitory effects of silver nanoparticles (AgNPs) on biofilm formation, a one-way analysis of variance (ANOVA) was conducted for each ESKAPE pathogen using OD_{590} values obtained from the biofilm quantification assays. The tested AgNP concentrations were 25, 50, 75, and 100 µg/mL, with untreated bacterial cultures serving as negative controls. The analysis revealed that AgNP concentration had a statistically significant effect on biofilm formation in *Enterococcus faecium* ($F = 6.58$, $p = 0.008$), *Staphylococcus aureus* ($F = 4.59$, $p = 0.026$), and *Acinetobacter baumannii* ($F = 4.95$, $p = 0.021$), indicating a dose-dependent inhibition of biofilm biomass in these strains. These results confirm the sensitivity of these pathogens to nanoparticle-mediated biofilm disruption. In contrast, the ANOVA results for *Klebsiella pneumoniae* ($F = 1.55$, $p = 0.258$), *Pseudomonas aeruginosa* ($F = 1.95$, $p = 0.180$), and *Escherichia coli* ($F = 1.79$, $p = 0.207$) did not reach statistical significance, despite observed trends toward reduced OD_{590} values at higher AgNP concentrations (Table 3). This lack of significance may be attributed to greater variability within treatment groups, possibly reflecting more robust or heterogeneous biofilm matrices and higher tolerance to AgNP exposure.

Table 3: One-Way ANOVA Summary Table. Statistical significance was determined using one-way ANOVA for OD_{590} values ($n = 3$). $p < 0.05$ indicates a significant difference across AgNP concentrations.

Pathogen	F	P-value	Significance
E. faecium	6.58	0.008	Significant
S. aureus	4.59	0.026	Significant
K. pneumonia	1.55	0.258	NS
A. baumannii	4.95	0.021	Significant
P. aeruginosa	1.95	0.180	NS
E. coli	1.79	0.207	NS

These findings are further corroborated by the percent inhibition data, where *S. aureus* exhibited the highest biofilm inhibition (61.71%) at 100 µg/mL, followed by *A. baumannii* (52.58%) and *P. aeruginosa* (48.50%) (Table 1). While *P. aeruginosa* showed relatively high inhibition in absolute terms, the variation among replicates likely reduced the statistical power to detect a significant difference. In summary, the statistical analysis supports the efficacy of green-synthesized AgNPs in disrupting biofilm formation, particularly in *S. aureus*, *A. baumannii*, and *E. faecium*. The species-specific differences in response underscore the complexity of biofilm behavior and highlight the importance of tailored approaches in evaluating and applying nanoparticle-based antimicrobials.

Conclusion

This work establishes a green approach for synthesizing silver nanoparticles (AgNPs) using *Acalypha godseffiana* leaf extract, resulting in small, stable, and biomolecule-capped nanostructures. The biosynthesized nanoparticles were confirmed through multiple characterization techniques and demonstrated promising biological activity against clinically important pathogens. Their mechanism of action appears linked to oxidative stress and biofilm disruption, suggesting their potential role in combating multidrug-resistant infections. Overall, these findings highlight *A. godseffiana*-mediated AgNPs as sustainable nanomaterials with strong potential for biomedical applications, particularly in infection control and therapeutic formulations. Future investigations will focus on evaluating *in vivo* efficacy, toxicity profiling, and formulation optimization, including synergistic combinations with conventional antibiotics for enhanced therapeutic outcomes.

Conflict of Interest

The authors declare no conflict of interest.

Authors' Declaration

The authors hereby declare that the work presented in this article is original and that any liability for claims relating to the content of this article will be borne by them.

Acknowledgements

This research was conducted as part of the requirements for the award of the Doctor of Philosophy (PhD) degree at Lovely Professional University (Phagwara), Punjab, India. The authors are grateful to all those who contributed to the successful completion of this work.

References

1. Patel RR, Kumar R, Bhatt P, Rawal R, Parikh A, Padalia H, Singh S. A novel nanotherapeutic approach: dual action of green-synthesized silver nanoparticles from *Clerodendrum serratum* against MDR-ESKAPE pathogens with wound healing potential. J Drug Deliv Sci Technol. 2025;108:106907.
2. Khan MH, Unnikrishnan S, Ramalingam K. Antipathogenic efficacy of biogenic silver nanoparticles and antibiofilm activities against multi-drug-resistant ESKAPE pathogens. Appl Biochem Biotechnol. 2024;196(4):2031–2052.
3. Mishra M, Ballal A, Rath D, Rath A. Novel silver nanoparticle-antibiotic combinations as promising antibacterial and anti-biofilm candidates against multiple-antibiotic resistant ESKAPE microorganisms. Colloids Surf B Biointerfaces. 2024;236:113826.
4. Yassin MT, Mostafa AAF, Al-Askar AA, Al-Otibi FO. Synergistic antibacterial activity of green synthesized silver nanomaterials with colistin antibiotic against multidrug-resistant bacterial pathogens. Crystals. 2022;12 (8):1057.
5. Raza S, Wdowiak M, Grotek M, Adamkiewicz W, Nikiforow K, Mentea P, Paczesny J. Enhancing the antimicrobial activity of silver nanoparticles against ESKAPE bacteria and emerging fungal pathogens by using tea extracts. Nanoscale Adv. 2023;5(21):5786–5798.
6. Bhatia P, Sharma A, George AJ, Anvitha D, Kumar P, Dwivedi VP, Chandra NS. Antibacterial activity of medicinal plants against ESKAPE: an update. Heliyon. 2021;7(2):e06310.
7. Ali AY, Alani AAK, Ahmed BO, Hamid LL. Effect of biosynthesized silver nanoparticle size on antibacterial and anti-biofilm activity against pathogenic multi-drug resistant bacteria. OpenNano. 2024;20:100213.
8. Luzala MM, Muanga CK, Kyana J, Safari JB, Zola EN, Mbusa GV, Nuapia YB, Liesse JMI, Nkanga CI, Krause RWM, Balčiūnaitienė A, Memvanga PB. A critical review of the antimicrobial and antibiofilm activities of green-synthesized plant-based metallic nanoparticles. Nanomaterials. 2022;12(11):1841.
9. Olubodun SO, Eriyamremu GE, Ayevbuomwan ME, Nzoputa CI. In vitro antioxidant activity and phytochemical analyses of *Acalypha godseffiana* (Euphorbiaceae) leaf extracts. Niger J Nat Prod Med. 2021;25(1):75–79..
10. Oni MO, Akinmoladun FA, Olajuyigbe OO, Ogunwande IA, Olawale FA. Insecticidal and toxicological study of n-hexane leaf extract of *Acalypha godseffiana* used as a protectant for wheat grains. Eur J Zool Res. 2019;7(1):19–29.
11. Samreen, Roy DN, Ahmad I. Chapter 4 - Combating biofilm of ESKAPE pathogens from ancient plant-based therapy to modern nanotechnological combinations. In: Roy DB, editor. Advances in Cancer Stem Cells. Academic Press; 2022;20:59–94.
12. Hossain, M. R., Biplob, A. I., Sharif, S. R., Bhuiya, A. M., & Sayem, A. S. M. Antibacterial Activity of Green Synthesized Silver Nanoparticles of Lablab purpureus Flowers Extract against Human Pathogenic Bacteria. Trop. J. Nat. Prod. Res. 2023; 7(8): 3647–3651.
13. Swidan NS, Hashem YA, Elkhatib WF, Yassien MA. Antibiofilm activity of green-synthesized silver nanoparticles against biofilm-associated enterococcal urinary pathogens. Sci Rep. 2022;12(1):1–13.
14. Mohanta YK, Biswas K, Jha SK, Hashem A, Abd Allah EF, Mohanta TK. Anti-biofilm and antibacterial activities of silver nanoparticles synthesized by the reducing activity of phytoconstituents present in the Indian medicinal plants. Front Microbiol. 2020;11(6):1–15.
15. Azimzadeh M, Sabziparvar B, Jafari A, Noorbakhsh F, Kazemzadeh A, Rahbar M. Biofilm inhibition of multidrug-resistant *Pseudomonas aeruginosa* using green-synthesized silver nanoparticles and colistin. Sci Rep. 2025;15(1):14993.
16. Labulo AH, David OA, Terna AD. Green synthesis and characterization of silver nanoparticles using *Morinda lucida* leaf extract and evaluation of its antioxidant and antimicrobial activity. Chem Pap. 2022;76(12):7313–7325.
17. Dada AO, Adekola FA, Dada FE, Adelani-Akande AT, Bello MO, Okonkwo CR, Inyinbor AA, Oluyori AP, Olayanju A, Ajanaku KO, Adetunji CO. Silver nanoparticle synthesis by *Acalypha wilkesiana* extract: phytochemical screening, characterization, influence of operational parameters, and preliminary antibacterial testing. Heliyon. 2019;5(10):e02517.
18. Khanal LN, Sharma KR, Paudyal H, Parajuli K, Dahal B, Ganga GC, Pokharel YR, Kalauni SK. Green synthesis of silver nanoparticles from root extracts of *Rubus ellipticus* Sm. and comparison of antioxidant and antibacterial activity. J. Nanomater. 2022;2022(1):1–12.
19. Pramasari N, Anjani AG, Muslikh FA, Lestari TP, Shoviantari F, Septyaningrum SD, Melati IS, Randy GY. Green Synthesis, Optimization and Characterization of Carrot Extract Silver Nanoparticles. Trop J Nat Prod Res. 2024;8(12):9591–9595 .
20. Halilu, E. M., Ngweh, V. A. & Airemwen, C. O. Green Synthesis of Silver Nanoparticles from Parinari curatellifolia Methanol Stem Bark Extract and Evaluation of Antioxidant and Antimicrobial Activities. Trop. J. Nat. Prod. Res. 2023;7(3), 2498–2505.
21. Bernardes LMM, Malta SM, Santos ACC, Silva RA, Rodrigues TS, da Silva MNT, Bittar VP, Borges ALS, Justino AB, Nossol ABS, Martins MM, Espíndola FS, Mendes-Silva AP, Ueira-Vieira C. Green synthesis, characterization, and antimicrobial activity of silver nanoparticles from water-soluble fractions of Brazilian kefir. Sci. Rep. 2025;15(1):1–18.
22. Panda MK, Dhal NK, Kumar M, Mishra PM, Behera RK. Green synthesis of silver nanoparticles and their potential effect on phytopathogens. Mater Today Proc. 2021;35(2):233–238.
23. Banerjee P, Satapathy M, Mukhopahayay A, Das P. Leaf extract mediated green synthesis of silver nanoparticles from

widely available Indian plants: synthesis, characterization, antimicrobial property and toxicity analysis. Bioresour. Bioprocess. 2014;1(3):1–10.
24. Umar Z, Bello UR, Mathur A, Tailor G, Chaudhary J, Singh S. Modulation of biofilm with synthesized silver nanoparticles from *Azadirachta indica*. Curr Res Green Sustain Chem. 2021;4:100203.
25. Rabochova M, Lorin J, Černíková A. Antibiofilm activity of silver nanoparticles biosynthesized using viticultural waste. PLoS ONE. 2022;17(8):e0272844.
26. Xie Y, Wang L, Yang Y, Zha L, Zhang J, Rong K, Tang W, Zhang J. Antibacterial and anti-biofilm activity of diarylureas against Enterococcus faecium by suppressing the gene expression of peptidoglycan hydrolases and adherence. Front Microbiol. 2022;13(12):1071255.
27. Artono A, Purnami N, Handoko E, Widodo AD, Juniastuti J. Pseudomonas aeruginosa in chronic suppurative otitis media. Infect Chemother.. 2018; 57(1):63-71.
28. Sulthana RN, Rajanikanth A. Green synthesis of silver nanoparticles using seed extract of *Foeniculum vulgare* and their antibacterial activity. Int J Curr Res Biosci Plant Biol. 2018;5(7):77–83.
29. Keskin C, Aslan S, Baran MF, Baran A, Eftekhari A, Adıcan MT, Ahmadian E, Arslan S, Mohamed AJ. Green synthesis and characterization of silver nanoparticles using Anchusa officinalis: antimicrobial and cytotoxic potential. Int J Nanomedicine. 2025;20(4):4481–4502.
30. Corciovă A, Mircea C, Burlec AF, Fifere A, Moleavin IT, Sarghi A, Tuchilus C, Ivănescu B, Macovei I. Green synthesis and characterization of silver nanoparticles using a Lythrum salicaria extract and in vitro exploration of their biological activities. Life. 2022;12(10):1643 .
31. Fagbemi K, Thonda O, Daramola O, Oyewole O, Adeduro S, Popoola D, Aina A. Antibacterial activity of silver nanoparticles synthesized using Vitex grandifolia against multidrug-resistant (MDR) pathogens. Trop J Nat Prod Res. 2024;8(8):8068–8074.
32. Vicencio-Salas Solís C, Zavaleta-Mancera HA, García-Díaz SE, García-Nava R, Trejo-Téllez LI, Robledo-Paz A. Green synthesis of silver nanoparticles using Cedrela odorata and their fungicidal activity against Fusarium circinatum. J Nanopart Res. 2024;26(7):1-15
33. Gwada CA, Ndivhuwo PS, Matshetshe K, Aradi E, Mdluli P, Moloto N, Otieno F, Airo M. Phytochemical-assisted synthesis, optimization, and characterization of silver nanoparticles for antimicrobial activity. RSC Adv. 2025;15(18):14170–14181.
34. Niluxsshun MCD, Masilamani K, Mathiventhan U. Green synthesis of silver nanoparticles from the extracts of fruit peel of *Citrus tangerina, Citrus sinensis,* and *Citrus limon* for antibacterial activities. Bioinorg Chem Appl. 2021;2021(1), 6695734.
35. Rajak KK, Pahilani P, Patel H, Kikani B, Desai R, Kumar H. Green synthesis of silver nanoparticles using Curcuma longa flower extract and antibacterial activity. 2023;1(4)1–20.
36. Castañeda-Aude JE, Morones-Ramírez JR, De Haro-Del Río DA, León-Buitimea A, Barriga-Castro ED, Escárcega-González CE. Ultra-small silver nanoparticles: a sustainable green synthesis approach for antibacterial activity. Antibiotics. 2023;12(3):574
37. Chandrasekaran M, Chinnaiyan U, Sivaprakasam S, Paramasivam S. Biogenic synthesis and characterization of silver nanoparticles using a combined leaf extract for antibacterial and biofilm inhibition properties. Trop J Nat Prod Res. 2025;9(3):1089–1096.
38. Merghni A, Lassoued MA, Noumi E, Hadj Lajimi R, Adnan M, Mastouri M, Snoussi M. Cytotoxic activity and antibiofilm efficacy of biosynthesized silver nanoparticles against methicillin-resistant Staphylococcus aureus strains colonizing cell phones. Can J Infect Dis Med Microbiol. 2022;2022(3):1–10.
39. Almatroudi A. Biofilm resilience: molecular mechanisms driving antibiotic resistance in clinical contexts. Biology (Basel). 2025;14(2): 165.
40. Siddique MH, Aslam B, Imran M, Ashraf A, Nadeem H, Hayat S, Khurshid M, Afzal M, Malik IR, Shahzad M, Qureshi U, Khan ZUH, Muzammil S. Effect of silver nanoparticles on biofilm formation and EPS production of multidrug-resistant *Klebsiella pneumoniae*. Biomed Res Int. 2020;2020(4):1–11.
41. Holubnycha V, Husak Y, Korniienko V, Bolshanina S, Tveresovska O, Myronov P, Holubnycha M, Butsyk A, Borén T, Banasiuk R. Antimicrobial activity of two different types of silver nanoparticles against a wide range of pathogenic bacteria. Nanomaterials. 2024;14(2):137.
42. Habash MB, Goodyear MC, Park AJ, Surette MD, Vis EC, Harris RJ. Potentiation of tobramycin by silver nanoparticles against *Pseudomonas aeruginosa* biofilms. Antimicrob Agents Chemother. 2017;61(10):15-17.
43. Asma ST, Imre K, Morar A, Imre M, Acaroz U, Shah SRA, Hussain SZ, Arslan-Acaroz D, Istanbullugil FR, Madani K. Natural strategies as potential weapons against bacterial biofilms. Life. 2022;12(10):1618.